THE NUCLEATION BEHAVIOR OF $K_2O \cdot TiO_2 \cdot 3GeO_2$ UNDERCOOLED MELT

SNEŽANA. R.GRUJIĆ, NIKOLA.S. BLAGOJEVIĆ, MIHAJLO. B.TOŠIĆ*,
VLADIMIR.D. ŽIVANOVIĆ*, JELENA. D.NIKOLIĆ*

Faculty of Technology and Metallurgy, 4 Karnegijeva St., 11000 Belgrade, Serbia
**Institute for Technology of Nuclear and other Mineral Raw Materials, 86 Franchet d' Esperey, 11000 Belgrade, Serbia*

E-mail: grujic@tmf.bg.ac.yu

The nucleation of $K_2TiGe_3O_9$ crystals in an undercooled melt of stoichiometric composition was studied. Volume nucleation with spherical morphology of the growing crystals was determined. The nucleation range is in the temperature interval 540-630°C. A maximum of the steady state nucleation rate of $I^{max} = 1.4 \times 10^{15}$ $m^{-3} \cdot s^{-1}$ was determined at the temperature $T_n^{max} = 582°C$. The temperature and time dependence of the nucleation rate was analyzed and it was shown that such a nucleation behavior was the result of a low thermodynamic and kinetic barrier. The results showed that the temperature intervals of nucleation and crystal growth of this undercooled melt partly overlapped.

INTRODUCTION

Germanium-containing glasses have received increased interest due to their technological applications, for example, in optical fibers or nonlinear optical devices, in which these materials are used as glasses or as transparent crystallized glasses. In both cases, knowledge of the processes occurring during glass crystallization is essential. Crystallization commences with nucleation, i.e., with the formation of crystal-like embryos, which are able to grow further. Embryos smaller than a critical size disappear whereas larger ones grow. Therefore, the conditions under which the process of nucleation is evolved are the most important for designing the microstructure. From the structural point of view, a fine-grained microstructure develops in a glass at a high nucleus density. This can be achieved by homogenous nucleation. Homogeneous nucleation is stochastic process occurring with same probability in volume. Knowledge of crystal nucleation is important not only for understanding the stability of glasses in practical applications, where the formation of nuclei and subsequent crystal growth must be avoided, but also to enable the preparation of crystallized glass with the desired microstructure and properties by controlled nucleation and growth.

In previous studies, some thermal properties and the crystallization mechanism of $K_2O \cdot TiO_2 \cdot 3GeO_2$ [KTG_3] glass were reported [1, 2]. X-Ray diffraction (XRD), analyses of heat treated KTG_3 glass revealed the formation of a $K_2TiGe_3O_9$ crystalline phase, indicating polymorphic crystallization (a crystalline phase having the same composition as the parent glass). Recently, Fukushima et al. [3] investigated the electronic polarizability and crystallization of $K_2O–TiO_2–GeO_2$ glasses. They also reported that the formed crystalline phase had the composition $K_2TiGe_3O_9$.

In the present study, the nucleation of $K_2TiGe_3O_9$ crystals in undercooled melt was investigated. The usual procedures were employed to determine the nucleation rates [4-8]. The measurements were performed on isothermally heated glass samples by scanning electron microscopy (SEM).

EXPERIMENTAL

The KTG_3 glass was prepared by melting a homogeneous mixture of reagent grade K_2CO_3, TiO_2 (both Fluka Chemica) and GeO_2 (electronic grade) in a platinum crucible. The melting was performed in an electric furnace with a temperature control of ±1°C at $T = 1300°C$ during $t = 2$ h. The glass was obtained by quenching the melt on a steel plate. Powder X-ray diffraction analysis (XRD) confirmed the quenched melts to be vitreous. The glass samples were transparent, without visible residual gas bubbles.

The experiments under isothermal conditions were performed on bulk samples. On the basis of the results of previous investigations [1, 2], a single-stage heating schedule was chosen. The glass samples were heated at a heating rate ß = 10°C/min up to the temperature of the heat treatment and maintained at the chosen temperature for different times. The treatment temperatures, T, and times, t, used in this study are given in Table 1.

After the selected heat treatment, the samples were taken out of the furnace. Sections fracture through the samples were gold sputtered and examined by SEM using a Jeol JSM 6460 microscope. From the SEM micrographs, the number of particles per unit area, N_A, and the diameters of the circular intersections of the particles were determined. The number of particles per unit volume, N_V, was determined from ratio of N_A and the largest circular cross-section diameter, d, [5, 8-10]. To determine N_V for each selected heat treatment, 3-10 samples were analyzed. Based on these measurements Nv was estimated as an average value. The nucleation rate, I, at the treatment temperature, T, was determined from the time dependence of the number of particles (spherulites) per unit volume, N_V, in the heat treated glass samples.

RESULTS

Taking into account the error in chemical analysis the glass with composition close to nominal one was obtained (Table 2).

Table 1. Heat treatment temperatures, T, and times, t, used for the determinations of the crystal nucleation rates.

T (°C)	t (min)								
540	200	250	300	360	100				
560	70	80	90	100	110	120	150		
580	25	30	33	35	38	40	43	45	48	50
590	15	20	25	30	35	40			
600	10	15	20	25	30				
610	10	15	20						
620	10	30							
640	1000								

In previous investigations of the crystallization of this glass, it was shown that during heat treatment a $K_2TiGe_3O_9$ crystalline phase was formed [1, 2].

Single-stage heat treatment was chosen on the basis of the results of numerous investigations of the microstructure of samples heat treated under different treatment conditions. The fact that the number of particles per unit area, N_A, can be measured directly after a single-stage heat treatment at T indicates that the crystal growth rates in the temperature interval of nucleation have considerable values.

Selected SEM micrographs are presented in Figure 1. It is obvious that the nucleation process commences within the bulk of the heat treated glasses and that the morphology of the growing crystals is spherical.

The time dependence of N_V measured from SEM micrographs of samples heat treated at 540, 560, 580, 590 and 600°C are shown in Figure 2a-e, respectively. The slopes of these dependences correspond to the nucleation rate at the heat treatment temperature.

The steady state crystal nucleation and growth rates as a function of temperature are presented in Figure 3, from which it can be seen that the temperature intervals of nucleation and crystal growth of this undercooled melt partly overlapped. The value of the maximum steady-state crystal nucleation rate is $I^{max} \approx 1.4 \times 10^{15}$ m⁻³ s⁻¹ at 582°C. This value belongs to one of the highest values of the nucleation rate of a crystalline phase determined in inorganic glasses.

Table 2. Chemical analysis of the KTG₃.

	Oxide, x_i (mol.%)		
	GeO₂	K₂O	TiO₂
Nominal	60	20	20
Analyzed	58	19	22
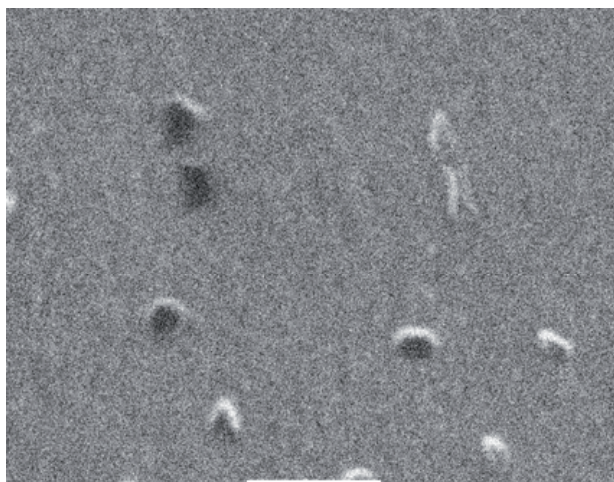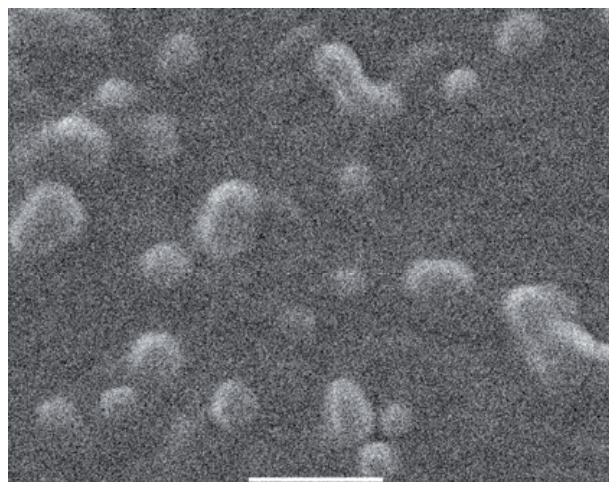
Figure 1. SEM micrographs of crystallized samples of KTG₃ after heat treatment at: a) T = 580°C for t = 38 min and b) T = 580°C for t = 48 min.

DISCUSSION

Analysis of the temperature dependent nucleation rate

According to the classical nucleation theory, an embryo is enlarged atom by atom until a critical nucleus is assembled. A critical nucleus is stable and capable of further growth. For polymorphic nucleation of a spherical nucleus with a sharp interface between the viscous melt and with the same properties as the corresponding macro-phase, assuming a temperature independent crystal/liquid interfacial energy, the steady state crystal nucleation rate, *I*, is given as a function of absolute temperature, *T*, by [8, 10-13]:

$$I = A \exp(-\frac{W*}{kT}) \exp\left(-\frac{\Delta G_D}{kT}\right) \qquad (1)$$

where *A* is the pre-exponential factor, *W** is the thermodynamic free energy barrier to nucleation, ΔG_D is the kinetic free energy barrier for transport of a 'formula unit' from the melt to a nucleus and *k* is the Boltzmann constant.

In a narrow temperature range (100-200°C), as is the nucleation range for most glasses, *A* can be approximated by [14]:

$$A = n_V kT / h \qquad (2)$$

where n_V is the number of 'formula units' of the nucleating phase per unit volume and *h* is Planck's constant.
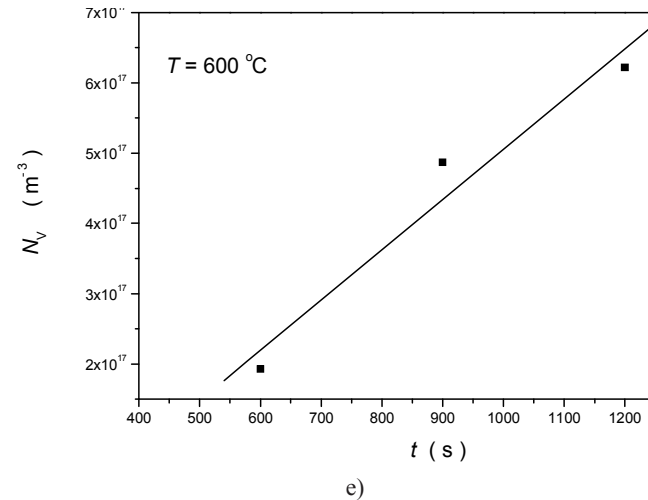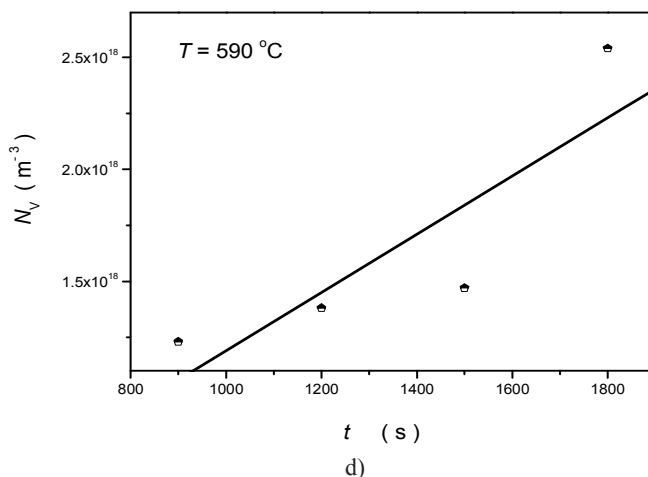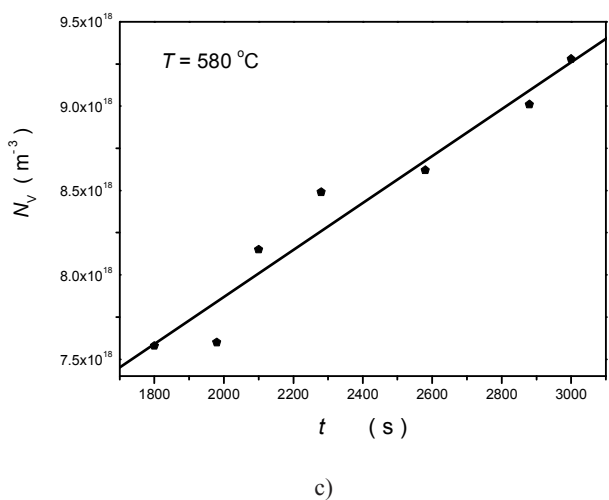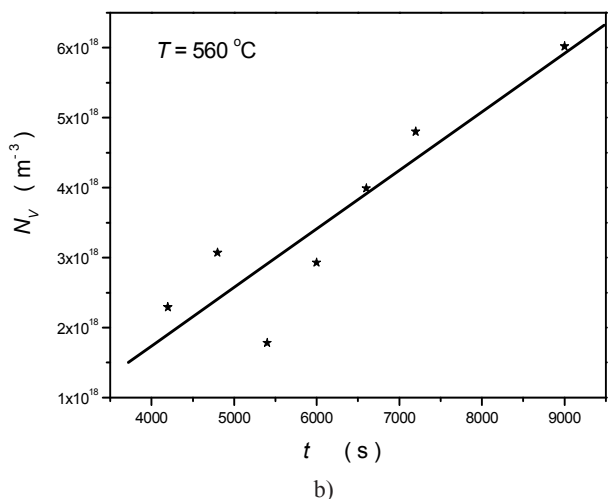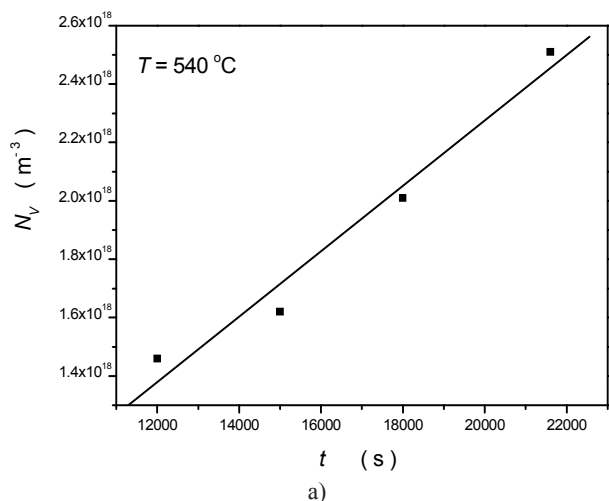

Figure 2. The number of particles per unit volume, N_V, as a function of time at the heat treatment temperature: a) 540°C; b) 560°C; c) 580°C; d) 590°C and e) 600°C. The solid lines correspond to the fit of the experimental points.

For a spherical nucleus, the thermodynamic free energy barrier to nucleation, W^*, is given by:

$$W^* = \frac{16\pi\sigma^3 V_m^2}{3\Delta G^2} \qquad (3)$$

where V_m, σ and ΔG are, respectively, the molar volume of the crystalline phase, the crystal/liquid interfacial energy and the free energy of crystallization (the free energy difference in the transformation liquid-crystal, i.e., the thermodynamic driving force for crystallization).

The kinetic barrier to nucleation, ΔG_D, can be expressed in terms of an effective diffusion coefficient:

$$D = \frac{kT\lambda^2}{h}\exp\left(-\frac{\Delta G_D}{kT}\right) \qquad (4)$$

where λ is the jump distance (of the order of atomic/molecular dimensions). For a complex oxide liquid, where molecular transport is a complicated atomic process, D can be related to the viscosity η through the Stokes-Einstein relation:

$$D = \frac{kT}{3\pi\lambda\eta} \qquad (5)$$

The temperature dependence of the glass viscosity is given by:

$$\eta = \eta_o \exp\left(\frac{\Delta G_\eta}{kT}\right) \qquad (6)$$

where ΔG_η is the activation free energy for viscous flow. According Equation (5), the activation free energies for diffusion and viscous flow are similar, i.e., $\Delta G_D \cong \Delta G_\eta$.

If in Equation (1), A is replaced with Equation (2), W^* with Equation (3) and $\exp(-\Delta G_D/kT)$ with the glass viscosity through Equations (4) and (5), the steady state crystal nucleation rate is given by:

$$I = \frac{n_v kT}{3\pi\lambda^3\eta}\exp\left(-\frac{16\pi\sigma^3 V_m^2}{3k}\frac{1}{\Delta G^2 T}\right) \qquad (7)$$

Equation (7) was used in the further analysis of the nucleation behavior of the KTG$_3$ phase. To calculate the theoretical steady state crystal nucleation rate of the
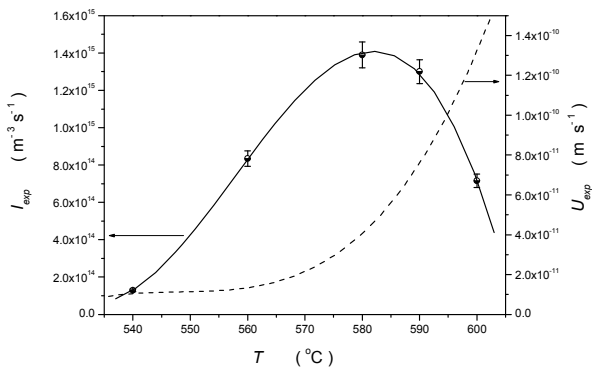
KTG$_3$ phase, according Equation (7), the parameters ΔG and σ must be known. The exact temperature dependence of ΔG can be calculated if the heat capacities of the liquid and crystal are known as a function of temperature. However, the heat capacity of an undercooled liquid is commonly unavailable. For this reason, the temperature dependence of ΔG was estimated from [15]:

$$\Delta G = -\frac{\Delta H_m}{T_m}(T_m - T) - \int_T^{T_m}\Delta C_p dT + T\int_T^{T_m}\left(\frac{\Delta C_p}{T}\right)dT \qquad (8)$$

where ΔH_m is the melting enthalpy, T_m is the melting temperature of the crystal and ΔC_p ($\Delta C_p < 0$) is the difference between heat capacities of the crystalline and liquid phases at constant pressure at a temperature T. If $\Delta C_p = const.$ in the investigated temperature interval, integration of Equation (8) yields

$$\Delta G = -\frac{\Delta H_m}{T_m}(T_m - T) + \Delta C_p\left[(T_m - T) - T\ln\left(\frac{T_m}{T}\right)\right] \qquad (9)$$

To calculate ΔG according to Equation (9), data from DSC measurements were employed. Parameter $\Delta C'_p$ ($\Delta C'_p = -\Delta C_p$) was determined using the relation $\Delta C'_p \approx (\Delta H_m - \Delta H_c)/(T_m - T_c)$,

The glass viscosities were obtained from the empirical Vogel-Fulcher-Tamann equation (VFT), which describes well the temperature dependence for most glasses [9, 24]. The VFT equation was fitted using the glass transformation temperature, T_g, the dilatometric softening temperature, T_{om}, and the melting temperature, T_m, determined by dilatometric and DSC measurements [1], Table 3.

The lack of a direct method for measuring the surface energy of the nucleus/undercooled melt interface, σ, is the problem for the determination of this parameter. The parameter σ is treated as a macroscopic property with a value equal to the respective value for a planar interface. This assumption is known as the capillarity approximation. As a suitable method for the determination σ is its calculation from experimental nucleation rate data [14]. Accordingly, Equation (7) was linearized. Using the experimental data for the nucleation rate, the plot of $\ln(I\eta/T)$ against $1/(T\Delta G^2)$ for KTG$_3$ is presented in Figure 4. The obtained straight line indicates good agreement of the experimental data for I

Figure 3. Experimental steady-state nucleation rate, I, and growth rates, U, of KTG$_3$ phase in the temperature interval 540-600°C .

Table 3. The parameters of KTG$_3$ for estimated I_{theo}.

K (JK^{-1})	1.380622×10^{-23}	[19]
λ (m)	5.6×10^{-10}	[20]
n_v (m^{-3})	5.69×10^{27}	
V_m (m^3 mol^{-1})	123.6×10^{-6}	[21]
σ (T) (J m^{-2})	$\sigma(T) = -0.0233 + 1.576 \times 10^{-4}\,T$; T(K)	
ΔG (J mol^{-1})	$\Delta G(T)= -102.97(1308.16 - T) + 108.27$ $[(1308.16 - T) - T(\ln(1308.16/T))]$; T(K)	
η (Pas)	$\log\eta = -0.286 + 1739/(T - 684)$; T(K)	[2]

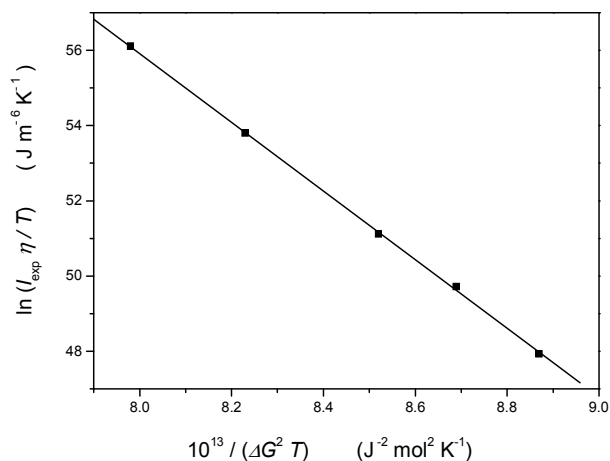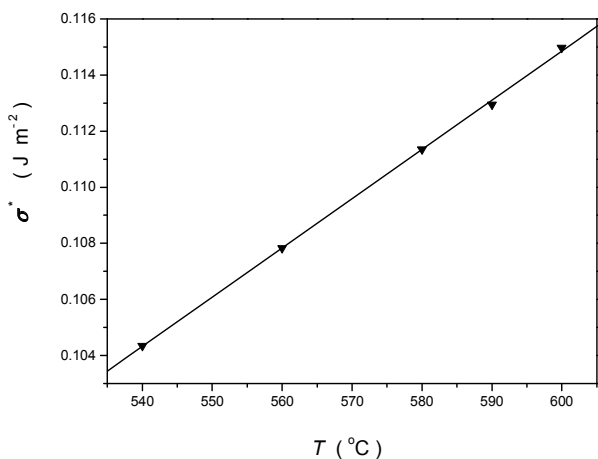Figure 4. ln($I\eta/T$) versus $1/(T\Delta G_2)$ plot for KTG$_3$.

Figure 5. Calculated crystal/liquid interfacial energy, σ c, according to Equation (7) with $A_{c,theo}$ and I_{exp} as a function of temperature.
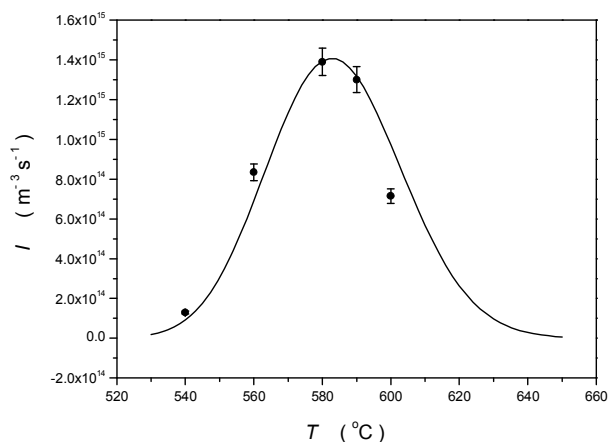

Figure 6. Experimental(●) and calculated nucleation rate (—) according to Equation (7) with the data from Table 3 as a function of temperature.

with theory within the investigated temperature range. From the slope of the plot, the temperature independent crystal/liquid interfacial energy was found to be σ = 0.170 Jm^{-2}.

From the intercept of the plot, the pre-exponential factor $A_{c,exp}$ = 9.49×10^{55} Jm^{-6}K^{-1} was determined. However, this value is in strong disagreement with the theoretical pre-exponential value $A_{c,theo} = n_v k/3\pi\lambda^3$ 4.75×10^{31} Jm^{-6}K^{-1}. A similar discrepancy was obtained for other (silicate) glasses [8, 9].

The discrepancy between the experimental and theoretical values of A_c can be avoided if σ is calculated from the experimental values of the nucleation data (*I*) and η, employing the theoretical value of $A_{c,theo}$. According to this method, the values of σ^c at the selected temperatures were calculated from Equation (7) and plotted in Figure 5, from which it can be seen that σ weakly increases with increasing temperature (dσ/d*T* = = 1.576×10^{-4} Jm^{-2} K^{-1} in the range 540-600°C). This value of the temperature coefficient σ is in the range of the highest ones hitherto calculated. An increase of σ with increasing temperature was obtained for other glasses (dσ/d*T* ≈ (0.06-0.16)×10^{-3} Jm^{-2}K^{-1}), regardless of the manner of estimating the kinetic barrier [8, 9]. The increase of the surface tension with increasing temperature is in conflict with the theoretical provisions. From a thermodynamic point of view, a decrease of σ (for planar interfaces) with temperature is to be expected [16]. It follows that a contradiction exists between the discussed interpretation of the experimental results and the general theoretical expectations. This contradiction can be partly removed by taking into account a possible dependence of the surface energy on the size of a nucleus [17]. Another possible explanation is a local increased ordering of the melt in the vicinity of a nucleus, which could lead to a decrease of entropy and increase of the surface energy [12]. According to certain non-classical nucleation theories [18], the assumption of a sharp crystal/liquid interface is questionable and as a result of this assumption the positive temperature dependence of σ appears.

Using the values of the parameters from Table 3 in Equation (7), the theoretical nucleation rate of KTG$_3$ crystals was calculated and compared with the experimental nucleation rates in Figure 6. From the rate of nucleation curve, the temperature at the maximum nucleation rate, T^{max}, is found to be 582°C, which is in agreement with experimentally determined value.

According to the classical nucleation theory, high nucleation rates can be expected in a system with small kinetic barriers and/or with small thermodynamic barriers. The kinetic barriers can be estimated through the viscosity and for this purpose, the viscosity at the temperature of the maximum nucleation rate was calculated to be 7.67×10^9 Pas, which allows diffusion and structural rearrangements required for crystal nucleation and growth. According to Equation (3) the

thermodynamic free energy barrier to nucleation, W^*, can be estimated through the crystal/liquid interfacial energy, σ, and thermodynamic driving force for crystallization, ΔG. Small values of σ indicate structural similarity of the crystal and the undercooled melt, small thermodynamic barriers and nucleation at a high nucleation rate.

To understand clearly the nucleation behavior of this undercooled melt, its nucleation parameters were compared with those of silicate glass Na$_2$O–2CaO–3SiO$_2$ (NC$_2$S$_3$), where the lower nucleation rate was determined. The nucleation rate of the NC$_2$S$_3$ was ~10^{11} m^{-3} s^{-1} [5, 9, 22]. Both undercooled melts crystallize by the homogenous mechanism.

The characteristic temperatures and parameters of the VFT equation, describing the dependence $\eta(T)$ for these glasses, are shown in Table 4.

In Figure 7 the $\eta(T)$ curves for the undercooled melts discussed above in the reduced temperature range $T_r = T/T_m = 0.5$-0.7 are presented.

If the VFT equation is a good approximation of the temperature dependence of viscosity for the KTG$_3$, it may be seen from Figure 7 that the viscosity of this

Table 4. Fulcher parameters and T_g, T_n^{max}, T_m for the KTG$_3$ and NC$_2$S$_3$.

Sample	C	B	T_o	T_g (K)	T_m (K)	T_g/T_m
KTG$_3$	-0.29	1739	411	823	1308	0.63
NC$_2$S$_3$	-4.86	4893.3	274.4	852	1562	0.54

Table 5. Parameters T_n^{max}, $\eta(T_n^{max})$, T_n^{max}/T_m and the nucleation range [T_N/T_m] for the KTG$_3$ and NC$_2$S$_3$.

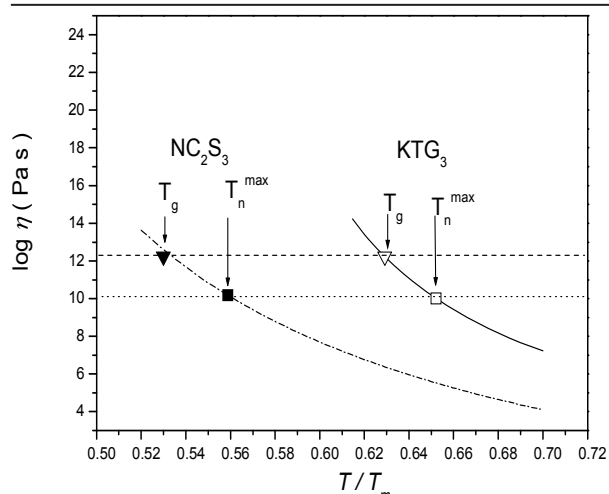| Sample	T_n^{max} (K)	T_n^{max}/T_m	$\eta(T_n^{max})$ (Pas)	Nucleation range (T_n/T_m)
KTG$_3$	855	0.65	0.8×10^{10}	0.62 - 0.70
NC$_2$S$_3$	873	0.56	1.5×10^{10}	0.54 - 0.60

Figure 7. Viscosity curves for KTG$_3$ and NC$_2$S$_3$ in the range $T_r = 0.5$-0.7. The points denote viscosity at the reduced temperatures of maximum nucleation rates (T_n^{max}) and glass transition temperature (T_g).

undercooled melt in the temperature range of $T_r = 0.5$-0.7 differs considerably from those of NC$_2$S$_3$. Its viscosity is higher and temperature dependence is strongly expressed. Also, considerable viscosity change with temperature occurs at $T_r > 0.55$. Consequently, T_g, T_n^{max} and nucleation interval are shifted to higher T_r, Table 5.

Based on experimental nucleation data for several silicate glasses [11, 23], it has been observed that glasses, which exhibit homogeneous nucleation have a reduced glass transition temperature T_{gr} ($T_{gr} = T_g/T_m$) < 0.60. As can be seen in Table 5, the glass NC$_2$S$_3$ has $T_{gr} < 0.6$ while the KTG$_3$ glass has $T_{gr} > 0.6$ (0.65). This indicates that the viscosity of this undercooled melt considerably influences the temperature and the time dependence of nucleation rate, as well as the shifting of T_n^{max} toward higher T_r values. The temperatures of the maximum nucleation rate, T_n^{max}, of these undercooled melts appeared at a viscosity of $\eta \approx 10^{10}$ Pas.

In Figure 8, W^*/kT as a function of the reduced temperature for these undercooled melts is shown. The values of W^*/kT were calculated from Equation (10) as:

$$W^*/kT = \ln A_c - \ln (I_{st}\eta/T) \qquad (10)$$

As can be seen in Figure 8, the values of W^*/kT for the KTG$_3$ were higher than those for the NC$_2$S$_3$. This is an opposite relation to that for the magnitude of their nucleation rates. For a detailed insight of the influence of this parameter on the nucleation rate according Equation (3), it is necessary to compare the thermodynamic driving forces, ΔG, and the surface energies, σ.

The dependencies of the thermodynamic driving forces, $\Delta G(T)$, versus the reduced temperature are shown in Figure 9. The values of $\Delta G(T)$ for the KTG$_3$ and NC$_2$S$_3$ undercooled melts were calculated using Equation (9).

As can be seen in Figure 9, $\Delta G(T)$ of KTG$_3$ has higher values than that of the NC$_2$S$_3$. The high thermodynamic driving force for crystallization of the KTG$_3$
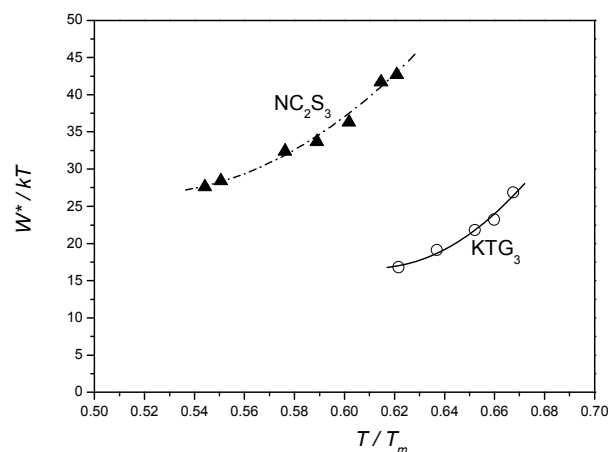

Figure 8. The thermodynamic barrier, W^*/kT, versus reduced temperature for KTG$_3$ and NC$_2$S$_3$.

is caused by its large melting enthalpy, Table 6.

It may be seen in Table 6 that the KTG$_3$ had a lower interfacial energy, σ and the reduced interfacial energy, α than the NC$_2$S$_3$. Previous investigations showed that for silicate glasses, which nucleate homogenously, the values of the reduced interfacial energy α are in the range of 0.40-0.55 [13, 27]. Taking into consideration possible experimental errors, it seems that the values of the reduced interfacial energy, α, of this germanate undercooled melt are not in the range of this parameter determined for silicate ones.

The complex relation between the thermodynamic driving force, ΔG, and the interfacial energy, σ, according to Equation (3) determines that the KTG$_3$ has a small value of the thermodynamic barrier, W^*. This indicates that W^* is the dominant factor determining the magnitude of the nucleation rate, I of the KTG$_3$, since the same relation exists as in the case of the magnitude of the nucleation rates, I, of these undercooled melts.

Analysis of the time dependent nucleation rate

The nucleation rate in an undercooled melt is time dependent until the time required for a steady state size distribution of the crystalline embryos is attained. This initial period is termed transient nucleation. The time dependent nucleation rate for the KTG$_3$ was estimated from the experimentally determined N_V. The induction times $t_{ind,exp}$ were determined by extrapolation of the linear part of the $N_V(t)$ plot to intersection with the time axis, t. The logarithm of the nucleation induction times, $t_{ind,exp}$, versus $1/T$ is plotted in Figure 10.

Kashichev [25] proposed the analytical solution for the transition time $τ$ for homogeneous nucleation as:

$$τ = \frac{8kT}{π^2 S_c \beta_c Z} \qquad (11)$$

where S_c is the surface area of the critical nucleus, $\beta_c = -(\partial^2 \Delta G_n / \partial n^2)_{nc}$ (ΔG_n is the Gibbs free energy required to form a cluster of n formula units and n_c refers to the critical nucleus) and Z is the number of formula units that join a critical nucleus per unit time per unit area. Only approximate numerical estimates of the transition times can be made from the above solution. There are uncertainties in the values of parameters such as σ and λ. Also in deriving the expressions for Z and $τ$, a simplified

Table 6. Interfacial energies, σ and σ(T), reduced interfacial energy, α, melting enthalpies ΔH$_m$, molar volumes V_m of the crystal phases and size of building units, λ.

Sample	σ (J m^{-2})	Average value of σ(T) (J m^{-2})	α	ΔH$_m$ (kJ mol^{-1})	$V_m \times 10^6$ (m^3 mol^{-1})	$λ \times 10^{10}$ (m)
KTG$_3$	0.170	0.109	0.264	134.70	123.60	5.60
NC$_2$S$_3$	0.174	0.118	0.406	91.12	126.60	5.88

Table 7. The values of transient times, τ, for the KTG$_3$ and NC$_2$S$_3$.

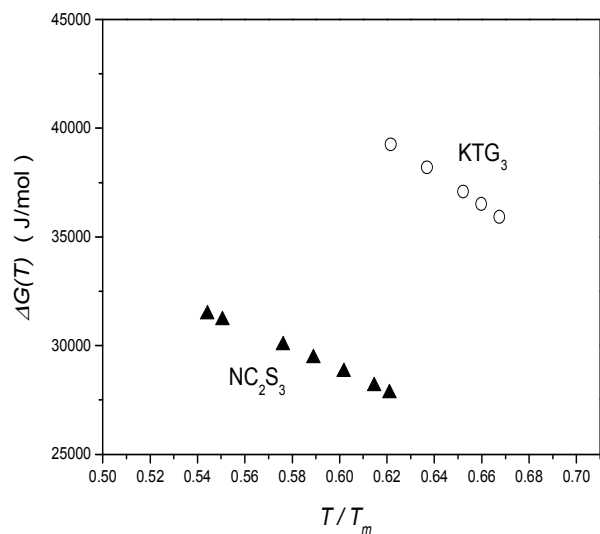| Sample	τ (s) in nucleation range	$τ_{T < Tn,max}$ (s)	$τ_{T,calcul}$ (s)	$τ_{T,exp}$ (s)
KTG$_3$	3.13×10^5 - 0.64	3.13×10^5 -182	239 ($T = 580°C$)	1014 ($T = 580°C$)
NC$_2$S$_3$	1.83×10^4 - 0.33	1.83×10^4 -618	305 ($T = 607°C$)	623 ($T = 607°C$)

Figure 9. Thermodynamic driving force ΔG(T) for KTG$_3$ and NC$_2$S$_3$ versus reduced temperature.
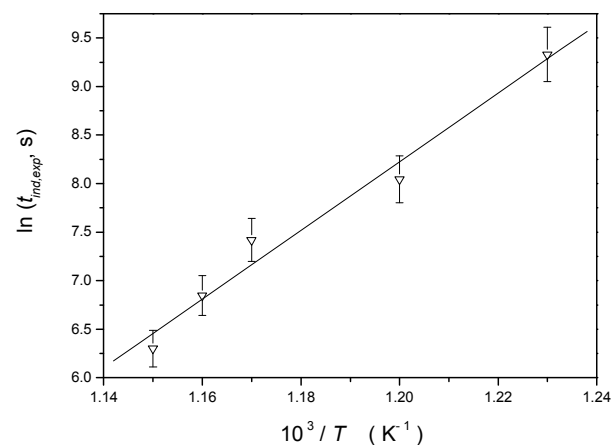

Figure 10. The logarithm of the induction period, $t_{ind,exp}$ versus $1/T$. The straitght line is least square fit.

model is used involving diffusion by a jump process. When $t \to \infty$ it follows that $t_{ind} = (\pi^2/6) \times \tau$. However, the actual processes occurring in the interface region and the nature of the species involved are unknown. James [26] rearranged Equation (11) and used the Stokes-Einstein equation to give:

$$\tau = \frac{48\sigma\lambda^5\eta N_a^2}{\pi D G} \qquad (12)$$

where N_a is the Avogadro's number.

By using the appropriate values from Tables 4 and 6 and Equation (12), the transient times, τ, for KTG₃ and NC₂S₃ in the reduced temperature range 0.5-0.7 were calculated. In Figure 11, it can be seen that the KTG₃ exhibited a stronger temperature dependence of the transient nucleation time than the NC₂S₃.

The transient times, τ, in the nucleation temperature range are presented in Table 7.

As seen in Table 7, KTG₃ has the higher transient time, τ, in the nucleation temperature range than of the NC₂S₃. Also, it can be seen from Table 7 that for the both undercooled melts the time dependence of nucleation rate appears at $T < T_n^{max}$. At $T > T_n^{max}$, the transient times were very short, hence the time dependence of the nucleation rate in this temperature range was weak. For both undercooled melt, differences between $\tau_{Tn,calc}$ and $\tau_{T,exp}$ exist. For the KTG₃, τ_T at $T = 580°C$ is shown. The temperature $T = 580°C$ is the closest temperature below T_n^{max} (582°C) at which the nucleation rate was experimentally determined. Also, it may be seen that at this temperature, the experimentally determined transient time $\tau_{Tn,exp}$, is longer by one order of magnitude compared with the time calculated from Equation (12), $\tau_{T,calc}$. Except for experimental errors, the reason for this disagreement may be the Stokes-Einstein equation, which gives an error of one order of magnitude at temperatures near the transformation range.
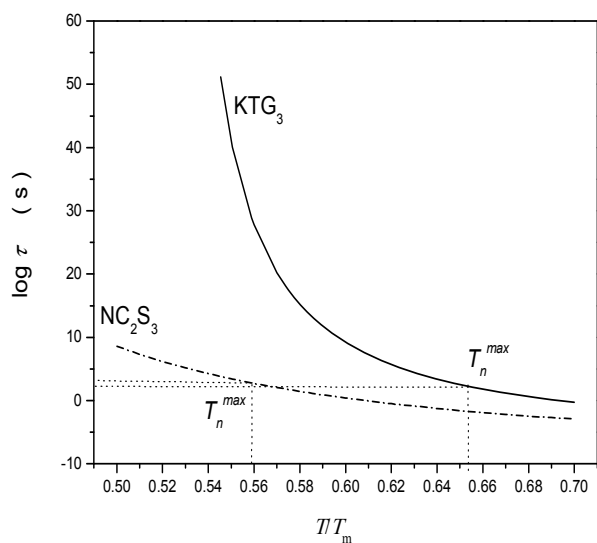
CONCLUSIONS

The crystal nucleation kinetics of K₂TiGe₃O₉ in an undercooled melt of stoichiometric composition was determined by SEM. It was detected that the nucleation commenced in the volume with spherical morphology of the growing crystals.

The nucleation occurs in the temperature range 540-630°C, and the results indicate that the temperature intervals of nucleation and crystal growth partly overlapped. The value of the steady state nucleation rate maximum is $I^{max} = 1.4 \times 10^{15}$ m⁻³ s⁻¹ at the temperature $T_n^{max} = 582°C$. Analysis of the results using the classical nucleation theory and the assumption that the crystal-liquid interfacial energy, σ, does not depend on temperature and the size of the nucleus, showed a good qualitative description of nucleation rate data, with a calculated $\sigma = 0.170$ J m⁻². However, the pre-exponential factor is about 24 orders of magnitude higher than the theoretical one. A better agreement between the experimental and theoretical values of the pre-exponential factor was obtained by using a temperature dependent interfacial energy, σ, the temperature coefficient of which was calculated to be $d\sigma/dT = 1.576 \times 10^{-4}$ J m⁻² K⁻¹.

Analysis of the time dependent nucleation rate showed that time dependence of the nucleation rate appeared at $T < T_n^{max}$. At $T > T_n^{max}$, the transient times were very short, thus, the time dependence of nucleation rate in this temperature range was weak

Also, the analysis showed that such a nucleation behavior of K₂O–TiO₂–3GeO₂ undercooled melt is a result of low thermodynamic and kinetic barriers.

Figure 11. The transient times, τ, calculated according to Equation (12) as a function of the reduced temperature for KTG₃ and NC₂S₃.

References

1. Grujić S., Blagojević N., Tošić M., Živanović V.: Ceramics-Silikáty *49*, 278 (2005).
2. Grujić S., Blagojević N., Tošić M., Živanović V., Božović B.: J. Therm. Anal. Calor. *83*, 463 (2006).
3. Fukushima T., Benino Y., Fujiwara T., Dimitrov V., Komatsu T.: J. Solid State Chem. *179*, 3949 (2006).
4. Zanotto E. D., Galhardi A.: J. Non-Cryst. Solids *104*, 73 (1988).
5. Gonzales Oliver C. J. R., James P.: Thermochim. Acta *280/281*, 223 (1996).
6. Zanotto E. D., James P. F.: J. Non-Cryst. Solids *124*, 86 (1990).
7. Zanotto E. D.: J. Mater. Res. *13*, 2045 (1998).
8. Fokin V., Zanotto E. D., Yuritsyn N. S., Schmelzer J. W. P.: J. Non-Cryst. Solids *352*, 2681 (2006).
9. Gonzales Oliver C. J. R., Russo D. O., James P. J.: Phys. Chem. Glasses *45*, 100 (2004).

10. James P. F.: Phys. Chem. Glasses *15*, 95 (1974).
11. James P. F.: J. Non-Cryst. Solids *73*, 517 (1985).
12. Weinberg M. C., Zanotto E. D., Manrich S.: Phys. Chem. Glasses *33*, 99 (1992).
13. Fokin V. M., Zanotto E. D., Schmelzer J. W.: J. Non-Cryst. Solids *321*, 52 (2003).
14. Rowlands E. G., James P. F.: Phys. Chem. Glasses *20*, 1 (1979).
15. Diaz-Mora N., Zanotto E. D., Fokin V. M.: Phys. Chem. Glasses *39*, 91 (1998).
16. Gutzow I., Kashchiev D., Avramov I.: J. Non-Cryst. Solids *73*, 477 (1985).
17. Fokin V. M., Zanotto E. D.: J. Non-Cryst. Solids *265*, 105 (2000).
18. Granasy L., James P.: J. Non-Cryst.Solids *253*, 2681 (1999).
19. Perry R. H., Green D. W., Maloney J. D.: *Perry`s Chemical Engeneers Handbook*, 6th ed., p. 256, McGraw-Hill, New York, 1984.
20. Henderson G. S., Wang H. M.: Eur. J. Mineral. *14*, 733 (2002).
21. JCPDS 27-0394.
22. Potapov O. V., Fokin V. M., Filipovich V. N.: J. Non-Cryst. Solids *247*, 74 (1999).
23. Zanotto E. D., Weinberg M. C.: Phys. Chem. Glasses *30*, 186 (1989).
24. Živanović V. D., Tošić M. B., Blagojević N. S., Grujić S. R., Mitrović M. M.: Ceramics-Silikáty *51*, 112 (2007).
25. Kashchiev D.: Surf. Sci. *14*, 209 (1969).
26. James P.F.: Phys.Chem.Glasses *15*, 95 (1974).
27. Cabral A. A., Fokin V. M., Zanotto E. D.: J. Non-Cryst. Solids *343*, 85 (2004).